Available online at www.sciencedirect.com
SCIENCE DIRECT
Journal of Power Sources 146 (2005) 204–208
JOURNAL OF POWER SOURCES
www.elsevier.com/locate/jpowsour

Electrochemical properties of nano-sized $Li_4Ti_5O_{12}$ powders synthesized by a sol–gel process and characterized by X-ray absorption spectroscopy

M. Venkateswarlu [a], C.H. Chen [a], J.S. Do [b], C.W. Lin [c], T.C. Chou [d], B.J. Hwang [a,*]

[a] *Department of Chemical Engineering, National Taiwan University of Science and Technology, Taipei 106, Taiwan, ROC*
[b] *Department of Chemical Engineering, Tunghai University, Taichung 704, Taiwan, ROC*
[c] *Department of Chemical Engineering, National Yunlin University of Science and Technology, Yunlin 640, Taiwan, ROC*
[d] *Department of Chemical Engineering, National Cheng Kung University, Tainan 700, Taiwan, ROC*

Available online 24 May 2005

Abstract

Nano-sized spinel $Li_4Ti_5O_{12}$ powders were synthesized by a sol–gel process. The cubic spinel structure without impurity phase of the synthesized $Li_4Ti_5O_{12}$ powders was confirmed by X-ray diffraction. The average grain size of the synthesized powders was found to be around 39 nm. In situ X-ray absorption spectroscopy (XAS) has been performed on the $Li_4Ti_5O_{12}$ electrode to investigate its change in the oxidation state and the local environment of the electrode during charging and discharging processes. The X-ray absorption near edge spectroscopy (XANES) analysis showed that the absorption edge energy shifts towards lower and higher energy, respectively, during discharge and charge processes, indicating the reversibility of the electrode is quite good. It was worthy to note that the discharging capacity and the charging capacity obtained for the nano-sized $Li_4Ti_5O_{12}$ electrode in the potential range of 0.01–1.75 V are 255 and 242 mAh g^{-1}, respectively. However, the specific charge capacity obtained in the potential range of 1.0–2.0 V is 126 mAh g^{-1}. The spinel $Li_4Ti_5O_{12}$ electrode maintains the cubic spinel structure for repeated cycling resulting in good cyclability and the capacity retention.

Keywords: Nano-sized; $Li_4Ti_5O_{12}$; XRD; XAS; Cycle performance

1. Introduction

Transition metal oxide materials have been identified as potential electrode materials for lithium-ion batteries because of their open structure and capability for accommodating guest ions [1–3]. However, many of the transition metal oxides exhibits high redox potentials (3–5.0 V versus Li) and more like cathode characteristics in nature. Only a few transition metal oxides shows low redox potential and good stability and one such oxide is lithium titanium oxide, $Li_4Ti_5O_{12}$ [1,2,4]. The main attractive features of this electrode are flat voltage profile and stable structure for repeated cycling [2–12]. In addition, the electrode materials are compatible to high voltage cathode materials and also solid polymer electrolytes [2,3,5–8]. Ohzuku et al. [4] have reported based on the X-ray diffraction analysis that there is no change in the unit cell volume of the $Li_4Ti_5O_{12}$ electrode during lithium insertion and extraction and it was named as zero strain material. An improvement in the shelf life and safety of the lithium-ion battery would be achieved using the $Li_4Ti_5O_{12}$ as an anode [2–8].

The co-existence of two phases, $Li_4Ti_5O_{12}$ and $Li_7Ti_5O_{12}$, has been observed based on the X-ray diffraction analysis by Scharner et al. [13]. Due to similar lattice constants of both phases and the low scattering factor of the lithium ions, the identification of the insertion mechanism using X-ray powder diffraction is possible only by using high angle X-ray scans. Ronci et al. [14] have reported that the insignificant change in the local environment with the insertion of lithium upon lithium intercalation based on the X-ray absorption spectroscopy (XAS) analysis. Within the discharge process,

* Corresponding author. Tel.: +886 2 27376624; fax: +886 2 27376644.
E-mail address: bjh@ch.ntust.edu.tw (B.J. Hwang).

0378-7753/$ – see front matter © 2005 Elsevier B.V. All rights reserved.
doi:10.1016/j.jpowsour.2005.03.016

the amplitudes of FT at Ti–Ti distance do not undergo any change until at least the insertion of lithium ions (x) up to 0.5. This followed by a significant reduction in the amplitude in the range of $0.5 < x < 0.7$. By $x = 0.75$, this change is saturated. They concluded that at least one intermediate step in the two-phase model proposed by Scharner et al. from the observed changes in XRD reflections needs to be included in the range of $0.5 < x < 0.7$ in the lithium insertion process.

It is believed that particle size and morphology have an influence on the cell performance of electrode materials. In particular, a decrease in mean particle size results in an increase in cyclability and rate capability of electrode materials because smaller particles are more flexible for lithium insertion/deinsertion than larger particles. Furthermore, during cycling the changes in the lattice parameters do not affect the cyclability of the smaller particles to the degree that larger particles are affected. Most of the electrochemical properties of the $Li_4Ti_5O_{12}$ electrodes reported are based on the corresponding powders prepared by solid-state reaction methods. It is known that solid-state reaction methods require an extensive mechanical mixing followed by high temperature grinding and sintering. Furthermore, solid-state reaction methods produce powders with large particle size, irregular shape and poor particle size distribution (PSD) resulting in poor electrochemical performance. The better electrochemical properties of $Li_4Ti_5O_{12}$ electrodes would be obtained if their corresponding powders with nano-sized particles, regular shape and uniform PSD can be obtained [8,11,12,15–17].

The synthesis and electrochemical properties of the nano-sized $Li_4Ti_5O_{12}$ particles prepared by a sol–gel process were investigated in this work. In situ XAS investigations was performed to elucidate the changes in the oxidation states and local environment of the electrode with the insertion and extraction of lithium ions during cycling processes.

2. Experimental

2.1. Preparation and characterization of electrode powders

A stoichiometric amount of titanium *iso*-propoxide and lithium acetate (Li/Ti = 4:5) were mixed in 75 mL of ethanol solvent and stirred at room temperature. The yellow colored solution turned to be white in color after stirring for 10 min. The temperature of the solution was raised to around 80 °C and stirred continuously till the formation of the gel. The gel was dried for 24 h at 60–70 °C in order to obtain the Li–Ti–O precursor powders. The Li–Ti–O precursor were ground to fine powder and calcined at 800 °C for 12 h in oxygen flowing condition to remove the presence of organic constituents.

The synthesized powder was characterized by X-ray diffraction (XRD) (Rigaku X-ray diffractometer, Rotaflex). XRD spectra were recorded with Cu Kα (λ = 1.5406 Å) radiation in the diffraction angle of 2θ from 10 to 100° at a scan rate of 5° min^{-1}. The grain size of the $Li_4Ti_5O_{12}$ powder was determined using Scherrer's formula [18] and the average grain size was found to be around 39 nm.

2.2. Preparation of electrode films and electrochemical measurements

The $Li_4Ti_5O_{12}$ electrode films were prepared by mixing of active material, carbon black to enhance the electronic conductivity and poly-vinylidene fluoride (PVdF) as a binder in the ratio of 85:7.5:7.5 (w/w). *N*-Methyl pyrrolidiznone (NMP) was used as a solvent. The slurry obtained after mixing of active material, carbon black, PVdF with NMP solvent and stirring, the resulting slurry was coated on a copper current collector and dried for 2 h at 120 °C in order to remove the NMP solvent. The resulting electrode foil was roll-pressed and punched to a circular disc. The electrode films were preserved in argon filled dry box (Unilab, Mbruan) in which oxygen and moisture contents were maintained less than 1 ppm.

The charge and discharge measurements were performed on a coin-type cell. The coin cell was assembled using the $Li_4Ti_5O_{12}$ electrode as an anode and lithium metal as a counter electrode. An equal volume of the ethylene carbonate (EC) and diethyl carbonate (DEC) (1:1) solvent with 1 M lithium hexa-fluoro-phosphate ($LiPF_6$) salt was used as an electrolyte. The polypropylene membrane was soaked in an electrolyte for 24 h prior to use. All the weighing and assembling of the coin cell elements were performed in argon filled dry box. The electrochemical performance of the $Li_4Ti_5O_{12}$ electrode was evaluated in the potential range of 1.0–2.0 V or 0.01–1.75 V at room temperature using a programmable multi-channel battery tester (Maccor 2300).

2.3. X-ray absorption spectroscopy measurements

In situ X-ray absorption spectroscopy (XAS) measurements were performed at the beam line BL-17C of the National Synchrotron Radiation Research Center (NSRRC) at Hsinchu, Taiwan. The storage ring was operated with electron energy of 1.5 GeV and beam currents ranging from 100 to 200 mA. A Si (1 1 1) double monochromatic crystal was employed for energy selection and higher order harmonic contamination was eliminated by mirrors. The intensity of the incident and transmitted beams were collected by gas ionization chambers as detectors. The monitor and detector chambers were filled, respectively, with nitrogen and a mixture of argon and helium. The cell was placed in front of the window of the third ionization chamber and the beam size was limited to an area of 2 mm × 2 mm. The energy calibration was performed at each scans using a Ti metal foil as a reference and XAS signals were collected simultaneously at Ti K-edge in the transmission mode.

FEFFIT program was used by following the standard procedures to evaluate the XAS data. In the absorption spectrum,

the pre-edge and EXAFS regions were fitted by a straight line and cubic spline, respectively. The EXAFS function was obtained after subtracting the pre-edge background from the overall absorption spectrum and normalized with respect to the edge step. The normalized $\chi(E)$ was transformed from energy space to k space. The $\chi(k)$ data were k weighted by power 3 to compensate the damping of EXAFS oscillations and the higher k weighted $\chi(k)$ function would be nearly like monochromatic sine waves of the overall data. The normalized ($k^3\chi(k)$) function of Ti absorber in the k space ranging between 3.0 and 11.0 Å^{-1} and Fourier transformed (FT) to r-space in order to separate the signal contribution from different coordination shells.

3. Results and discussion

3.1. X-ray diffraction

The X-ray diffraction patterns of the synthesized $Li_4Ti_5O_{12}$ powders and the JCPDS pattern of cubic spinel structure are shown in Fig. 1, indicating that the patterns of the $Li_4Ti_5O_{12}$ powders are in good agreement with the JCPDS one. The synthesized $Li_4Ti_5O_{12}$ powder has a close packed array of $Fd\bar{3}m$ space group, which was confirmed based on the XRD peak indexing. The well-defined peaks in the XRD pattern for the synthesized powder confirm its phase purity and high degree of crystallinity.

3.2. X-ray absorption spectroscopy

In situ XAS measurements were performed at Ti K-edge to detect the changes of the local environment for the $Li_4Ti_5O_{12}$ electrode during lithium insertion and extraction processes. The charge–discharge curve obtained at 0.1 C in the potential range of 0.01–1.75 V is shown in Fig. 2, indicating that the discharge and charge capacity are around 255 and 242 mAh g^{-1}, respectively. The charge and discharge capacity are much higher than the theoretical one (175 mAh g^{-1}) estimated from the insertion of three lithium

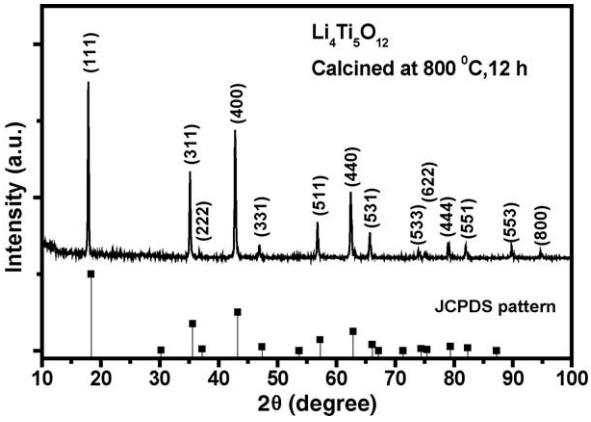

Fig. 1. XRD patterns of the $Li_4Ti_5O_{12}$ electrode powder.

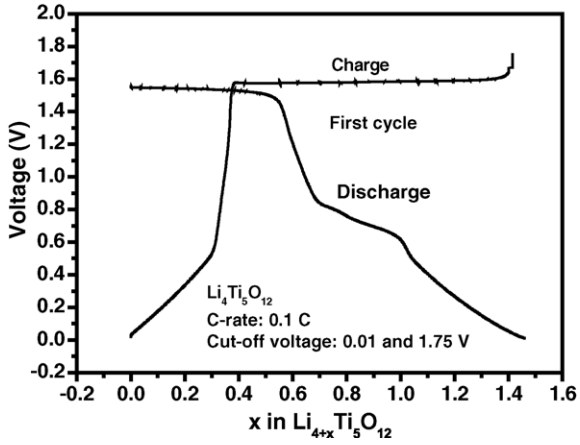

Fig. 2. Charge and discharge curves of the $Li_4Ti_5O_{12}$ electrode cycled at 0.1 C-rate.

ions, implying there are more than three lithium ions involving in the cycling process. This anomalous behavior needs to be further investigated. A plateau at around 1.5 V, which is in good agreement with the two-phase reaction between $Li_4Ti_5O_{12}$ and $Li_7Ti_5O_{12}$ proposed by Scharner et al. was observed. The discharge capacity (94 mAh g^{-1}) is much smaller than the charge capacity (175 mAh g^{-1}) at the plateau of 1.5 V. The charge capacity at the plateau of 1.5 V is consistent with the theoretical capacity for the extraction of three Li ions.

The normalized X-ray absorption near edge spectroscopy (XANES) and Fourier transform (FT) spectra at Ti K-edge for the $Li_4Ti_5O_{12}$ electrode during discharge process are presented in Fig. 3a and b. From Fig. 3a, it was found that the weak pre-edge peak at 4970 eV is corresponding to the transition of 1s → 3d unoccupied states which is electric dipole forbidden and quadruple allowed transition due to the mixing up of s and 4p states [19,20]. The transition of 1s to 4p involves a shakedown process. The features above the pre-edge peak at 4975 eV suggest the ligand to metal charge transfer (LMCT). As the lithium ion insertion process proceeds further, the ligand to metal charge transfer increases which means that the shakedown process dominates (Fig. 3a) and the lattice structure become closer. It could see from Fig. 3a that the absorption energy of the Ti K-edge gradually shifts towards lower energy region during lithium ion insertion process, indicating that the oxidation states of titanium were reduced. The change in the absorption energy during cycling process indicates that the electrochemical reactions are completely reversible. The following Eq. (1) explains the lithium ion insertion and extraction into and from the spinel oxide, respectively, during cycling processes:

$$Li_4Ti_5O_{12} + xLi^+ + xe^- \Leftrightarrow Li_{4+x}Ti_5O_{12} \quad (1)$$

From Fig. 3b, it can be observed that the FT magnitude (or distance) for the Ti–O shell and the Ti–Ti shell increases and decreases clearly, respectively, with an increase in x values in $Li_{4+x}Ti_5O_{12}$. However, Ronci et al. [14] have reported

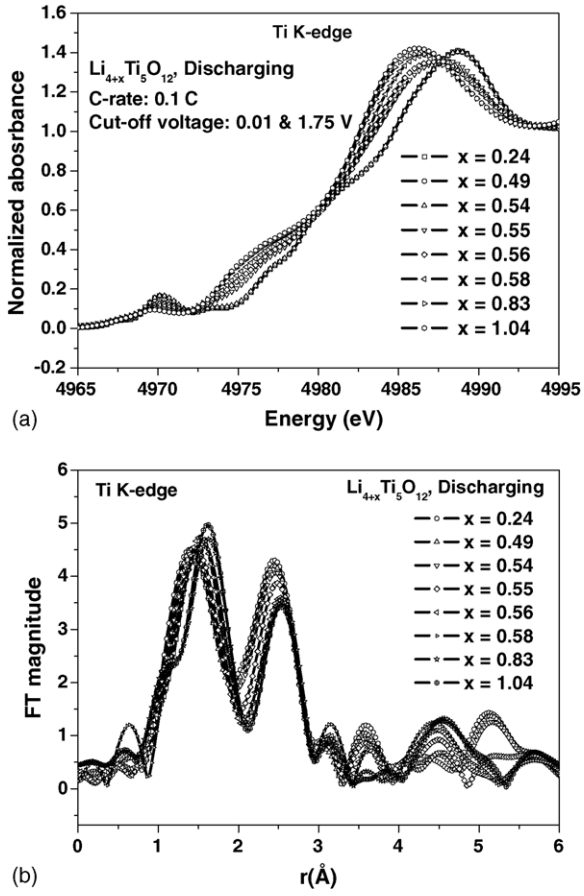

Fig. 3. (a and b) XANES and Fourier transformed spectra of Ti K-edge for the $Li_4Ti_5O_{12}$ electrode during discharging process.

that the FT magnitude and the distance for the Ti–O shell and Ti–Ti shell did not change upon discharge. Based on their data, they have concluded that at least one intermediate step needs to be included in the two-phase reaction. We believe that the reason responsible for this controversy is that the data quality at high k is not good enough to be analyzed in the Ronci et al.'s paper [14]. Our FT results showed that the obvious change of the Ti–Ti distance during Li intercalation suggests that the difference between the lattice parameters of the two phases should be large enough. However, Scharner et al. [13] have reported the difference between the lattice parameters for $Li_4Ti_5O_{12}$ (8.3595 Å) and $Li_7Ti_5O_{12}$ (8.3538 Å) is quite small. The EXAFS data needs to be further analyzed to understand this inconsistency and fitted to a suitable crystallographic model to elucidate the structural parameters, which would provide better view on the changes in the local environment of the electrode during cycling.

3.3. Electrochemical properties

To investigate the electrochemical properties of the nano-sized $Li_4Ti_5O_{12}$ electrodes at the plateau of 1.5 V, they

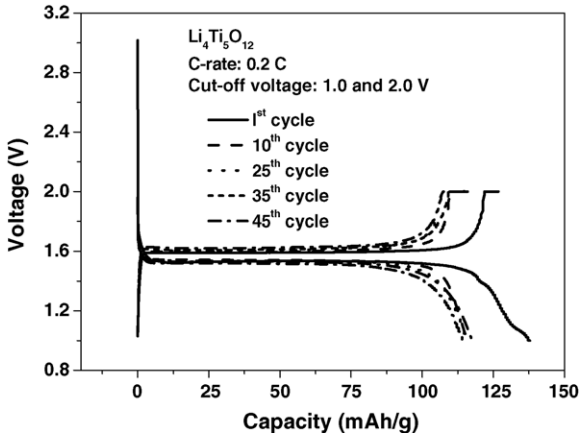

Fig. 4. Charge and discharge curves of the $Li_4Ti_5O_{12}$ electrode cycled at 0.2 C-rate.

are cycled at 0.2 and 0.5 C-rates in the potential range of 1.0–2.0 V. The charge–discharge curves of the $Li_4Ti_5O_{12}$ electrode at 0.2 C-rates are shown in Fig. 4. The irreversible capacity was observed only at the first cycle and there is no further capacity loss for the subsequent cycles. The charge capacity of 126 mAh g^{-1} was obtained with an average operating voltage at 1.56 V versus Li. During the discharge process, lithium ions are inserted into the host lattice with the co-existence of two phases ($Li_4Ti_5O_{12}$ and $Li_7Ti_5O_{12}$) [13]. The lithium ions are inserted into the $Li_{4+x}Ti_5O_{12}$ spinel structure and the inserted Li ions begin to occupy 8a and also empty 16c sites [4,10]. During the electrochemical reaction, the Li ions in the tetrahedral (8a) sites also migrate to 16c sites [4,9,10]. It seems all the lithium ions are moved to the 16c sites. The migration of all the lithium ions in the 16c sites, the anode still maintains cubic spinel structure, which shows the good structure stability and cyclability of the electrode. Fig. 5 shows the cycle tests for the $Li_4Ti_5O_{12}$ electrodes were performed at 0.2 and 0.5 C-rates. The capacity is slightly higher for 0.2 C-rates than at 0.5 C-rates and the capacity fading rates are 0.22 and 0.2 mAh g^{-1} per cycle, respectively,

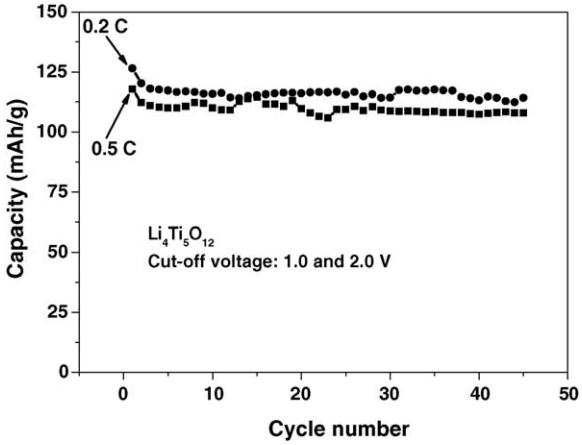

Fig. 5. Cyclability of the $Li_4Ti_5O_{12}$ electrode cycled at 0.2 and 0.5 C-rates.

at 0.2 and 0.5 C-rates. It indicates that the capacity retention and cyclability of the nano-sized $Li_4Ti_5O_{12}$ electrode are quite good due to its structure stability and flexibility during cycling.

4. Conclusion

The nano-sized $Li_4Ti_5O_{12}$ powders with high phase purity were synthesized successfully by a sol–gel process. The cubic spinel structure was identified based on the X-ray diffraction peak indexing and the average grain size was found to be 39 nm. The discharge and charge capacity were found to be around 255 and 242 mAh g^{-1}, respectively, at the potential range of 0.01–1.75 V at 0.1 C. The specific charge capacity of 126 mAh g^{-1} was obtained at 0.2 C with good capacity retention at the potential range of 1.0–2.0 V. The XANES results showed that the ligand to metal charge transfer increases during the discharge process suggests the shakedown process dominates and the lattice structure becomes close packed. It was worthy to note that the FT magnitude (distance) for the Ti–O shell and the Ti–Ti shell increases and decreases clearly, respectively, with an increase in x values in $Li_{4+x}Ti_5O_{12}$. The EXAFS data needs to be fitted to a suitable crystallographic model to extract the structural parameters, which would provide better view on the changes in the local environment of the electrode during cycling and the Li insertion–extraction mechanism.

Acknowledgements

The support from the Ministry of Education (Ex: 93-E-FA09-5-4) and also from NTUST, THU, NYUST, NCKU, Taiwan, is gratefully acknowledged.

References

[1] W.A. van Schalkwijk, B. Scrosati (Eds.), Advances in Lithium Ion Batteries, Kluwer Publications, New York, 2002.
[2] E. Ferg, R.J. Gummow, A. de Kock, M.M. Thackeray, J. Electrochem. Soc. 141 (1994) L147.
[3] P.P. Pier, M. Rita, P. Lorenzo, C. Vittoria, V. Paola, Solid State Ionics 144 (2001) 185.
[4] T. Ohzuku, A. Ueda, N. Yamamoto, J. Electrochem. Soc. 142 (1995) 1431.
[5] S. Panero, D. Satolli, M. Salomon, B. Scrosati, Electrochem. Commun. 2 (2000) 810.
[6] D. Peramunage, K.M. Abraham, J. Electrochem. Soc. 145 (1998) 2615.
[7] K. Zaghib, M. Armand, M. Gauthier, J. Electrochem. Soc. 145 (1999) 3135.
[8] A. Abouimrane, Y.A. Lebdeh, P.J. Alarco, M. Armand, J. Electrochem. Soc. 151 (2004) A1028.
[9] A.D. Robertson, L. Trevino, H. Tukamato, J.T.S. Irvine, J. Power Sources 81–82 (1999) 352.
[10] G.X. Wang, D.H. Bradhurst, S.X. Dou, H.K. Liu, J. Power Sources 83 (1999) 156.
[11] L. Kavan, M. Gratzel, Electrochem. Solid-State Lett. 5 (2002) A39.
[12] S. Bach, J.P. Pereira-Ramos, N. Baffier, J. Mater. Chem. 8 (1998) 251.
[13] S. Scharner, W. Weppner, P. Schmid-Beurmann, J. Electrochem. Soc. 146 (1999) 857.
[14] F. Ronci, P.E. Stallworth, F. Alamgir, T. Schiros, J.V. Sluytman, X. Guo, P. Reale, S. Greenbaum, M. denBoer, B. Scrosati, J. Power Sources 119–121 (2003) 631.
[15] B.J. Hwang, Y.W. Tsai, C.H. Chen, R. Santhanam, J. Mater. Chem. 13 (2003) 1962.
[16] B.J. Hwang, R. Santhanam, D.G. Liu, J. Power Source 101 (2001) 86.
[17] K. Nakahara, R. Nakajima, T. Matsushima, H. Majima, J. Power Sources 117 (2003) 131.
[18] B.D. Cullity, Elements of X-ray Diffraction, Addison-Wesley, 1956.
[19] H. Shigemura, M. Tabuchi, H. Sakaebe, H. Kobayashi, H. Kageyama, J. Electrochem. Soc. 150 (2003) A638.
[20] W.S. Yoon, C.P. Grey, M. Balasubramanian, X.Q. Yang, J. McBreen, Chem. Mater. 15 (2003) 3161.